

## The Crystal Structure of Synthetic $\text{Fe}_4^{2+}\text{Fe}_3^{3+}(\text{PO}_3\text{OH})(\text{PO}_4)_5$

*Ivo Vencato*

*Departamento de Física, Universidade Federal de Santa Catarina,  
88040-900 Florianópolis - SC, Brazil*

*Lígia de Farias Moreira and Enrico Mattievich*

*Instituto de Física, Universidade Federal do Rio de Janeiro  
21945-970 Rio de Janeiro - RJ, Brazil*

*Yvonne Primerano Mascarenhas*

*Instituto de Física e Química de São Carlos, USP, 13560-970 São Carlos - SP, Brazil*

Received: April 18, 1994

O novo composto sintético  $\text{Fe}_4^{2+}\text{Fe}_3^{3+}(\text{PO}_3\text{OH})(\text{PO}_4)_5$  é membro da série isoestrutural  $\text{Fe}_{7-x}^{2+}\text{Fe}_x^{3+}(\text{PO}_3\text{OH})_{4-x}(\text{PO}_4)_{2+x}$ , com  $x = 3$ , para  $0 < x < 4$ ,  $M_r = 961,2$ , triclínico, P-1,  $a = 7,971(1)$ ,  $b = 9,531(1)$ ,  $c = 6,389(2)$  Å,  $\alpha = 68,84(2)^\circ$ ,  $\beta = 78,40(2)^\circ$ ,  $\gamma = 66,93(1)^\circ$ ,  $V = 415,4(1)$  Å<sup>3</sup>,  $Z = 1$ ,  $D_x = 3,81$  Mg m<sup>-3</sup>,  $\lambda(\text{MoK}\alpha) = 0,71073$  Å,  $\mu = 63,8$  cm<sup>-1</sup>,  $F(000) = 448$ ,  $T = 298$  K,  $R = 0,050$  para 1299 reflexões observadas.

A estrutura consiste de íons de  $\text{Fe}^{2+}$  e  $\text{Fe}^{3+}$  coordenados por ligantes  $(\text{PO}_4)^-$  e  $(\text{PO}_3\text{OH})^{2-}$  formando cadeias poliédricas infinitas em zig-zag na direção  $[0 -2 0]$  e que compartilham arestas. Estas cadeias estão interligadas pelos vértices de octaedros de  $\text{Fe}^{2+}$  no centro da cela unitária e também por tetraedros de fosfatos. A proporção de íons de  $\text{Fe}^{3+}$  foi determinada por espectroscopia Mössbauer.

The new synthetic compound  $\text{Fe}_4^{2+}\text{Fe}_3^{3+}(\text{PO}_3\text{OH})(\text{PO}_4)_5$  is a member of the isostructural series  $\text{Fe}_{7-x}^{2+}\text{Fe}_x^{3+}(\text{PO}_3\text{OH})_{4-x}(\text{PO}_4)_{2+x}$ , with  $x = 3$ , for  $0 < x < 4$ ,  $M_r = 961.2$ , triclinic, P-1,  $a = 7.971(1)$ ,  $b = 9.531(1)$ ,  $c = 6.389(2)$  Å,  $\alpha = 68.84(2)^\circ$ ,  $\beta = 78.40(2)^\circ$ ,  $\gamma = 66.93(1)^\circ$ ,  $V = 415.4(1)$  Å<sup>3</sup>,  $Z = 1$ ,  $D_x = 3.81$  Mg m<sup>-3</sup>,  $\lambda(\text{MoK}\alpha) = 0.71073$  Å,  $\mu = 63.8$  cm<sup>-1</sup>,  $F(000) = 448$ ,  $T = 298$  K, final  $R = 0.050$  for 1299 observed reflections.

The structure consists of  $\text{Fe}^{2+}$  and  $\text{Fe}^{3+}$  ions coordinated by  $(\text{PO}_4)^-$  and  $(\text{PO}_3\text{OH})^{2-}$  ligands, forming infinite zig-zag polyhedral chains sharing edges along the direction  $[0 -2 0]$ . These chains are interconnected by the vertices of octahedral  $\text{Fe}^{2+}$  in the unit cell center and by phosphate tetrahedra. The  $\text{Fe}^{3+}$  ion proportion was determined by Mössbauer spectroscopy.

**Keywords:** iron phosphate, hydrothermal synthesis, Mössbauer

### Introduction

In a series of hydrothermal syntheses of iron phosphates under acidic conditions, dark brown-red prismatic crystals of mixed valence iron phosphate were obtained. Our sample, hereafter labeled S(41), is one member of an isostructural series,  $\text{Fe}_{7-x}^{2+}\text{Fe}_x^{3+}(\text{PO}_3\text{OH})_{4-x}(\text{PO}_4)_{2+x}$ , with  $0 < x < 4$ , where there is a continuous oxidation of the metal without destruction of the basic structure.

The chemical composition of this series was deduced from several members, obtained in different synthesis trials, where the initial composition of the ferrous and ferric phosphates were varied. The identification of the members of this series was done by X-ray diffraction on polycrystalline samples, and the  $\text{Fe}^{2+}$  and  $\text{Fe}^{3+}$  ion composition was determined using Mössbauer spectra. Due to the small amount of pure material isolated from each synthesis, it was not possible to estimate the chemical composition by direct

methods. Some syntheses gave single crystals with sufficiently good quality to perform X-ray diffraction analysis. We undertook X-ray data collection of four samples labeled S(27), S(19), S(41) and S(38). In this work we present the detailed crystal structure determination of the sample S(41) which showed the best refinement. We also establish a comparison of some crystallographic properties which vary with the composition of the four samples.

The synthesis of S(27) is similar to that of S(33), and in the case of S(33), with a composition rich in  $\text{Fe}^{2+}$  ( $x = 0$ ), that is  $\text{Fe}_{7-2x}(\text{PO}_3\text{OH})_4(\text{PO}_4)_2$ , the thermogravimetric analysis showed a loss of approximately four OH groups. With this information, it was possible to deduce the chemical composition of the sample S(41).

The hydrothermal synthesis of the sample S(41) was made by placing a quartz tube with a teflon cap containing

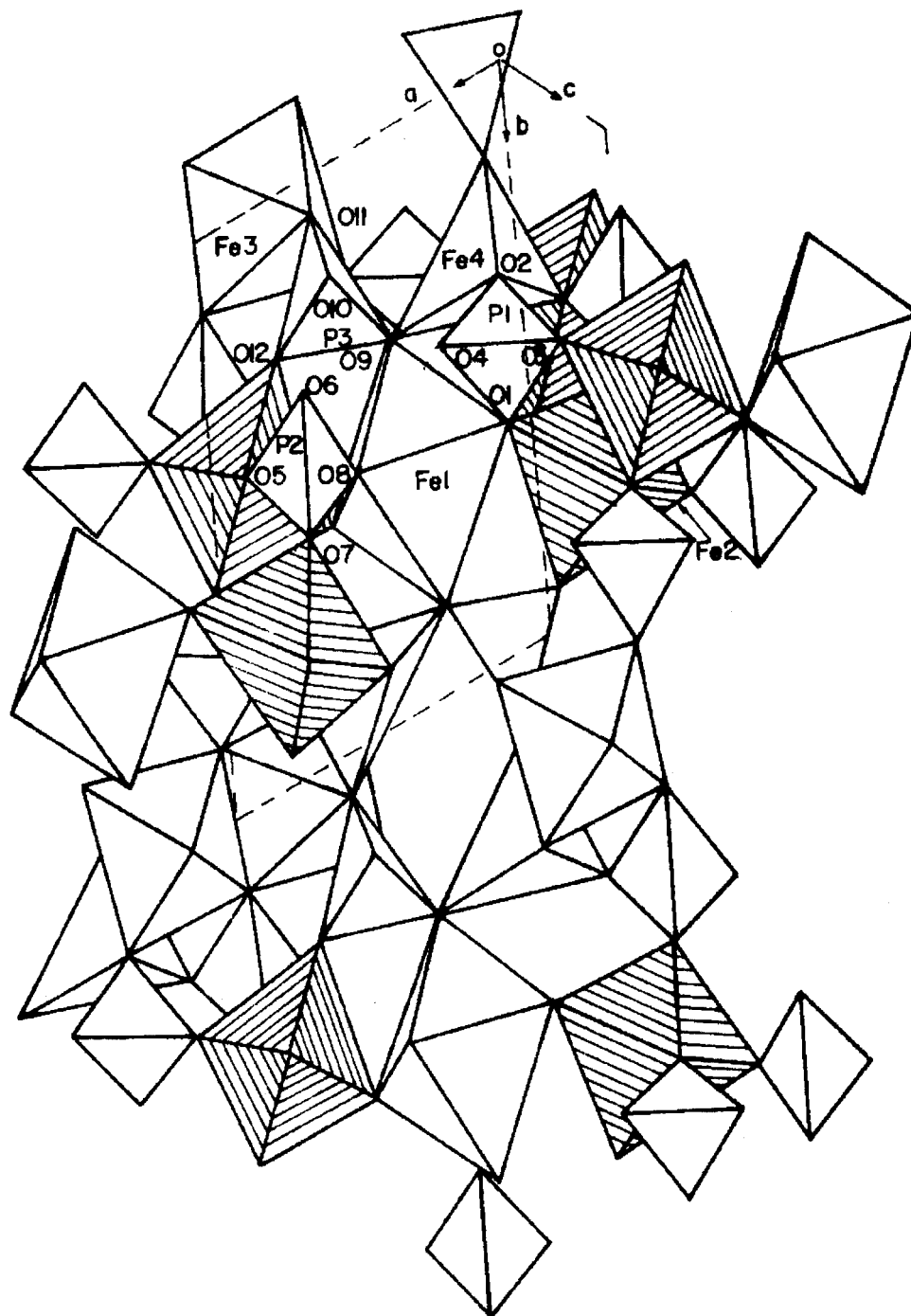


**Figure 1.** Polyhedral representation of the crystal structure of the S(41) iron phosphate with atomic labeling. The c-axis points out of the page. Only the Fe2 and Fe2' octahedra are ruled for easy identification.

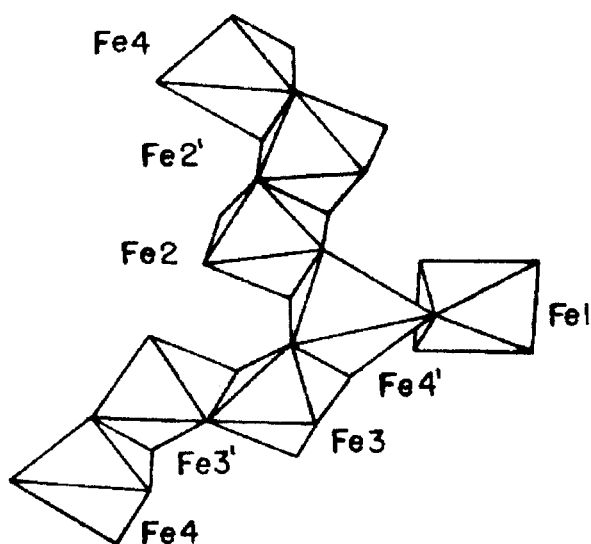


**Figure 2.** Schematic representation of the shared-edged polyhedral chain of the iron atoms. This view is slightly different from the previous projection. The primes designate the polyhedra generated by the inversion symmetry operation, without specifying the translations.

**Table 1.** Atomic coordinates and equivalent isotropic temperature factors for the S(41) iron phosphate.

Atom	x	y	z	$B_{\text{eq}} (\text{\AA})^2$
Fe(1)	0.5000	0.5000	0.5000	0.82(6)
Fe(2)	0.0485(1)	0.6100(1)	0.7715(1)	0.68(5)
Fe(3)	0.7796(1)	0.0255(1)	0.0187(1)	0.67(5)
Fe(4)	0.3116(1)	0.2154(1)	0.5054(2)	0.85(5)
P(1)	0.3504(2)	0.2684(2)	0.9601(3)	0.54(7)
O(1)	0.3028(5)	0.4394(4)	0.7875(6)	0.9(1)
O(2)	0.3132(5)	0.1574(4)	0.8621(6)	0.7(1)
O(3)	0.2336(5)	0.2740(4)	1.1833(6)	0.7(1)
O(4)	0.5505(2)	0.2048(5)	1.0010(6)	1.0(1)
P(2)	0.9062(5)	0.3322(2)	0.7594(2)	0.54(7)
O(5)	1.0353(5)	0.3350(4)	0.5414(6)	0.9(1)
O(6)	0.9487(5)	0.1545(4)	0.9104(6)	0.7(1)
O(7)	0.9593(5)	0.4145(4)	0.8934(6)	0.7(1)
O(8)	0.7117(5)	0.4183(5)	0.6966(6)	1.2(1)
P(3)	0.7333(2)	0.1260(2)	0.4713(3)	0.70(7)
O(9)	0.5433(5)	0.2570(4)	0.4681(6)	0.7(1)
O(10)	0.7892(6)	0.0299(5)	0.7118(7)	1.6(1)
O(11)	0.7358(5)	0.0050(5)	0.3603(6)	1.0(1)
O(12)	0.8696(5)	0.2076(5)	0.3379(7)	1.3(1)

$$*B_{\text{eq}} = \frac{4}{3} \sum_i \sum_j \beta_{ij} a_i \cdot a_j$$

equal parts of ferric acid phosphate and synthetic vivianite [ $\text{Fe}_3^{2+}(\text{PO}_4)_2(\text{H}_2\text{O})_8$ ], with water in a pressure vessel at 280 °C for one week. The ferric acid phosphate was obtained by adding, little by little, 26 g of ferric oxide ( $\alpha\text{-Fe}_2\text{O}_3$ ) to 120 g of boiling phosphoric acid ( $\text{H}_3\text{PO}_4$ ). The mixture was boiled for five hours, yielding a white precipitate. The synthetic vivianite was obtained using Evans's method<sup>1</sup>.

### Experimental Details

A prism-shaped crystal, 0.35 x 0.18 x 0.08 mm, was selected for intensity measurement on a CAD-4 Enraf-Nonius automatic diffractometer with monochromatic  $\text{MoK}\alpha$  radiation using a graphite monochromator. The unit cell parameters were derived from 25 reflections with a variable scan rate ( $7\text{-}20.0^\circ \text{min}^{-1}$ ) and two standard reflections ( $-3 \ -5 \ 1 \ e \ -4 \ -2 \ 3$ ) measured every 30 min without a significant change in intensities. The intensities were measured by the  $\theta$ - $2\theta$  scan technique with width  $(0.80 + 0.35 \tan \theta)^\circ$  and data collection performed with  $-8 < h < 9$ ,  $-9 < k < 11$ ,  $0 < l < 7$ . Of the 1631 measured reflections, 1465 were obtained after averaging Friedel pairs ( $R_{\text{int}} = 1.4\%$ ) and 1299 were observed with  $I > 3\sigma(I)$ . The intensities were corrected for the Lorentz-polarization factor, but no absorption correction was applied. An extinction correction was applied such that  $nz = 0.0157$  (SHELX76)<sup>2</sup>. The atomic scattering factors and the dispersion correction factors were taken from International Tables for X-ray Crystallography<sup>3</sup>.

The structure was solved by direct methods using the program MULTAN80<sup>4</sup>. The anisotropic refinement was made using full-matrix least-squares based on F. The function  $\sum w(1F_o - 1F_c)^2$  was minimized,  $w = [\sigma^2(F_o) + 0.005543 F_o^2]^{-1}$  where  $\sigma(F_o)$  is the estimated standard deviation for the observed amplitudes based on counting statistics. The refinement converged to  $R = 0.050$  ( $wR = 0.058$ ), with 170 varied parameters and a maximum of  $\Delta/\sigma = 0.60$ . The maximum peak height in the final Fourier synthesis was  $0.70 \text{ e \AA}^{-3}$  near the Fe(3) atom, probably due to the lack of absorption correction.

The SHELX76<sup>2</sup> program system was used with an IBM 3090 computer. The projections shown in Figs. 1 and 2 were calculated with the program ORTEP<sup>5</sup> incorporated in the Enraf-Nonius Structure Determination Package at the VAX computer facility of the Physics Department, Institute of Physics and Chemistry of São Carlos, University of São Paulo.

### Discussion and Conclusion

Atomic coordinates and equivalent isotropic thermal vibration parameters are given in Table 1, and polyhedral distances and angles in Table 2. The anisotropic thermal parameters are shown in Table 3. The Fe(1) atom is placed

**Table 2.** Polyhedral distances (Å) and angles (°) for the S(41) iron phosphate.

	<b>Fe(1)</b>				<b>Fe(2)</b>		
Fe(1)	- O(1)	2.228		Fe(2)	- O(1)	2.036	
	- O(8)	2.037			- O(7) <sup>B</sup>	2.086	
	- O(9)	2.283			- O(5) <sup>A</sup>	2.055	
	- O(1) <sup>A</sup>	2.228			- O(3) <sup>C</sup>	2.093	
	- O(8) <sup>A</sup>	2.037			-O(12) <sup>A</sup>	1.941	
	- O(9) <sup>A</sup>	2.283			- O(7) <sup>D</sup>	2.059	
average		2.183		average		2.045	
		O - O	O-Fe-O			O - O	O-Fe-O
O(1)	- O(8)	3.132	94.4	O(1)	- O(7) <sup>B</sup>	2.768	84.4
	- O(9)	3.040	84.7		- O(5) <sup>A</sup>	3.283	106.7
	- O(8) <sup>A</sup>	2.900	85.6		-O(12) <sup>A</sup>	2.954	95.9
	- O(9) <sup>A</sup>	3.333	95.3		- O(7) <sup>D</sup>	2.918	90.9
O(1) <sup>A</sup>	- O(8)	2.900	85.6	O(3) <sup>C</sup>	- O(7) <sup>B</sup>	2.663	79.2
	- O(9)	3.333	95.3		- O(5) <sup>A</sup>	2.619*	78.3
	- O(8) <sup>A</sup>	3.132	94.4		-O(12) <sup>A</sup>	3.104	100.6
	- O(9) <sup>A</sup>	3.040	84.7		- O(7) <sup>D</sup>	2.747	82.8
O(8)	- O(9)	3.214	95.9	O(7) <sup>B</sup>	- O(5) <sup>A</sup>	2.943	90.6
	- O(9) <sup>A</sup>	2.900	84.0		- O(7) <sup>D</sup>	2.778*	84.2
O(8) <sup>A</sup>	- O(9)	2.900	84.0	O(12) <sup>A</sup>	- O(5) <sup>A</sup>	2.828	90.2
	- O(9) <sup>A</sup>	3.213	95.9		- O(7) <sup>D</sup>	2.952	95.1
average		3.086	90.0	average		2.880	89.9
	<b>Fe(3)</b>				<b>Fe(4)</b>		
Fe(3)	-O(4) <sup>E</sup>	1.940		Fe(4)	- O(2)	2.144	
	-O(10) <sup>E</sup>	1.933			-O(5) <sup>B</sup>	2.054	
	-O(2) <sup>F</sup>	1.997			- O(9)	1.988	
	-O(6) <sup>E</sup>	2.030			-O(11) <sup>F</sup>	2.118	
	-O(11)	2.088			-O(3) <sup>E</sup>	2.085	
	- O(6) <sup>G</sup>	2.182					
average		2.028		average		2.078	
		O - O	O-Fe-O			O - O	O-Fe-O
O(4) <sup>E</sup>	-O(10) <sup>E</sup>	2.853	94.9	O(2)	-O(5) <sup>B</sup>	2.890	87.0
	- O(2) <sup>F</sup>	3.020	100.2		- O(9)	2.896	88.9
	-O(11)	2.661	82.6		-O(11) <sup>F</sup>	2.618*	75.8
	-O(6) <sup>E</sup>	2.985	97.5	O(3) <sup>E</sup>	-O(5) <sup>B</sup>	2.619*	78.5
O(6) <sup>G</sup>	-O(10) <sup>E</sup>	3.061	95.9		- O(9)	3.273	106.9
	- O(2) <sup>F</sup>	2.869	86.6		-O(11) <sup>F</sup>	3.133	96.4
	-O(11)	2.963	87.8	O(5) <sup>B</sup>	- O(9)	3.781	138.6
	-O(6) <sup>E</sup>	2.590*	75.8		-O(11) <sup>F</sup>	2.930	89.2
O(10) <sup>E</sup>	- O(2) <sup>F</sup>	2.829	92.1	O(9)	-O(11) <sup>F</sup>	3.712	129.4
	-O(6) <sup>E</sup>	2.749	87.8	O(2)	-O(3) <sup>E</sup>	4.186	163.7
O(11)	- O(2) <sup>F</sup>	2.618*	79.7				
	-O(6) <sup>E</sup>	3.186	101.3				
average		2.865	90.2	average		3.21	105.4

Table 2. (Continuation)

P(1)				P(2)			
P(1)	- O(1)	1.550		P(2)	- O(5)	1.555	
	- O(2)	1.549			- O(6)	1.554	
	- O(3)	1.544			- O(7)	1.555	
	- O(4)	1.508			- O(8)	1.501	
average		1.538		average		1.541	
		O - O	O-P-O			O - O	O-P-O
O(1)	- O(2)	2.525	109.2	- O(5)	- O(6)	2.518	108.2
	- O(3)	2.535	110.0		- O(7)	2.514	107.9
	- O(4)	2.486	108.8		- O(8)	2.490	109.2
- O(2)	- O(3)	2.534	110.0	- O(6)	- O(7)	2.475	105.5
	- O(4)	2.490	109.1		- O(8)	2.567	114.3
O(3)	- O(4)	2.497	109.8	O(7)	- O(8)	2.527	111.5
average		2.511	109.5	average		2.516	109.4
P(3)							
P(3)	- O(9)	1.538					
	-O(10)	1.529					
	-O(11)	1.550					
	-O(12)	1.524					
average		1.535					
		O - O	O-P-O				
O(9)	-O(10)	2.534	111.4				
	-O(11)	2.545	110.0				
	-O(12)	2.476	108.0				
O(10)	-O(11)	2.476	107.1				
	-O(12)	2.510	110.6				
-O(11)	-O(12)	2.498	108.7				
average		2.507	109.3				

Note: Estimated standard deviations for polyhedral distances and angles are 0.004 Å and 0.2°, respectively. A: 1-x, 1-y, 1-z; B: x-1, y,z; C: -x, 1-y, 2-z; D: 1-x, 1-y, 2-z; E: x,y,z-1; F: 1-x, -y, 1-z; G: 2-x, -y, 1-z; H: x,y,1+z; I: 1+x,y-1,z.

\* Shared edge.

in the center of the unit cell with a crystallographic occupancy factor of 1/2. The Fe(1), Fe(2) and Fe(3) atoms have octahedral coordination. The Fe(4) atom has a five-fold coordination with a distorted trigonal bipyramidal environment of oxygen atoms with oxidation state as a  $\text{Fe}^{2+}$  ion, as was also found by Moore<sup>6</sup> and Calvo<sup>7</sup> in the cases of the  $\text{Fe}_3(\text{H}_2\text{O})[\text{PO}_4]_2$  and the graftonite structures, respectively.

The structure represented in projection in Fig. 1 is formed by the Fe(2), Fe(3) and Fe(4) polyhedra sharing edges in infinite chains along the direction [0 -2 0]. In this Figure, the octahedra Fe(2) and Fe(2)' are ruled for easy identification. The sequence of iron atoms in the chain follows the scheme ... Fe(4)- Fe(3)'- Fe(3)- Fe(4)'- Fe(2)-

Fe(2)'- Fe(4)- ..., where the primes refer to the polyhedra generated by the inversion symmetry operation, without specifying the translations, as shown in the slightly different perspective of Fig. 2.

The Fe(1) octahedron shares corners with four equatorial oxygen atoms [O(1) of Fe(2), O(1)' of Fe(2)', O(9) of Fe(4) and O(9)' of Fe(4)'] and two apical oxygen atoms [O(8) of P(2) and O(8)' of P(2)']. This fact is the most striking feature of the structure: the Fe(1) octahedron connects four infinite chains of zigzag, shared edged polyhedra. Each of the  $\text{PO}_4$  tetrahedra shares the four corners with different Fe polyhedra.

**Table 3.** Anisotropic temperature factors for S(41).

Atom	U(1,1)	U(2,2)	U(3,3)	U(2,3)	U(1,3)	U(1,2)
Fe(1)	0.0070(6)	0.0062(5)	0.0155(6)	-0.0043(4)	-0.0039(5)	0.0023(4)
Fe(2)	0.0079(4)	0.0043(4)	0.0114(4)	-0.0030(4)	-0.0030(4)	0.0016(4)
Fe(3)	0.0084(4)	0.0052(4)	0.0112(4)	-0.0041(3)	-0.0009(3)	-0.0001(3)
Fe(4)	0.0068(5)	0.0116(4)	0.0123(4)	-0.0054(4)	-0.0016(4)	0.0004(4)
P(1)	0.0057(6)	0.0028(6)	0.0091(6)	-0.0030(5)	-0.0003(5)	0.0026(5)
O(1)	0.012(1)	0.006(1)	0.012(1)	-0.003(1)	0.001(1)	0.001(1)
O(2)	0.008(1)	0.008(1)	0.009(1)	-0.0037(9)	-0.001(1)	0.000(1)
O(3)	0.007(1)	0.006(1)	0.009(1)	-0.0022(9)	0.002(1)	0.002(1)
O(4)	0.008(1)	0.013(1)	0.016(1)	-0.007(1)	-0.004(1)	0.003(1)
P(2)	0.0065(7)	0.0034(6)	0.0092(6)	-0.0036(5)	-0.0010(5)	0.0014(5)
O(5)	0.012(1)	0.009(1)	0.010(1)	-0.005(1)	-0.001(1)	0.000(1)
O(6)	0.009(1)	0.007(1)	0.009(1)	-0.005(1)	-0.001(1)	0.000(1)
O(7)	0.007(1)	0.009(1)	0.009(1)	-0.003(1)	-0.003(1)	0.000(1)
O(8)	0.010(1)	0.015(1)	0.018(1)	-0.006(1)	-0.005(1)	0.001(1)
P(3)	0.0076(7)	0.0055(6)	0.0127(6)	-0.0071(5)	-0.0029(5)	0.0036(5)
O(9)	0.006(1)	0.005(1)	0.016(1)	-0.0061(9)	-0.002(1)	0.0033(9)
O(10)	0.028(1)	0.012(1)	0.020(1)	-0.009(1)	-0.008(1)	-0.001(1)
O(11)	0.014(1)	0.011(1)	0.014(1)	-0.007(1)	-0.008(1)	0.001(1)
O(12)	0.014(1)	0.023(1)	0.017(1)	-0.012(1)	0.003(1)	-0.007(1)

**Table 4.** Mössbauer parameters of the S(41) powder sample at 80 K fitted with line width of 0.279(2) mm/s for all sites.

	Intensity (mm/s)	Q.S. (mm/s)	I.S. (mm/s)	Relative Intens. (%)
Fe <sup>2+</sup> (1)	0.040(1)	1.7992(5)	1.460(2)	10.5
Fe <sup>2+</sup> (2)	0.040(1)	3.122(7)	1.242(1)	10.5
Fe <sup>2+</sup> (3)	0.060(1)	2.438(6)	1.447(2)	15.7
Fe <sup>2+</sup> (4)	0.080(1)	2.580(5)	1.203(1)	21.0
Fe <sup>3+</sup> (1)	0.080(1)	0.177(10)	0.244(8)	5.5
Fe <sup>3+</sup> (2)	0.021(2)	1.008(4)	0.312(1)	19.4
Fe <sup>3+</sup> (3)	0.074(1)	0.610(2)	0.373(1)	17.3

Q. S. = Quadrupole Splitting; I. S. = Isomer Shift

The shortest distance between metal atoms is along the chains, with Fe(2)-Fe(2)<sup>i</sup> = 3.077 Å, where i = -x, 1-y, 1-z, and the average distance of 3.334 Å suggests a good probability of electron transfer along the chains, as seen in the lipscombite structure<sup>8</sup>.

The average octahedral Fe<sup>2+</sup>-O and tetrahedral P-O distances are within the values of well-refined structures. The Fe-O distances of Fe(2) and Fe(3) have intermediate values between 1.933 and 2.182 Å, compatible with the occupation of irons with both valences in these sites. The

interatomic angles reveal great distortions of the octahedra, varying from O(6)<sup>G</sup>-Fe(3)-O(6)<sup>E</sup> = 75.8° to O(1)-Fe(2) - O(5)<sup>A</sup> = 106.7°, where the superscript letters designate the symmetry operations of Table 2. The shared edges of the polyhedral chains are among the shortest and the corresponding Metal-O distances are the longest, which is consistent with the cation-cation repulsion effects. It is possible to verify in Table 2 that the average Fe(1)-O distance is the longest, consistent with the oxidation state Fe(1) = Fe<sup>2+</sup>.

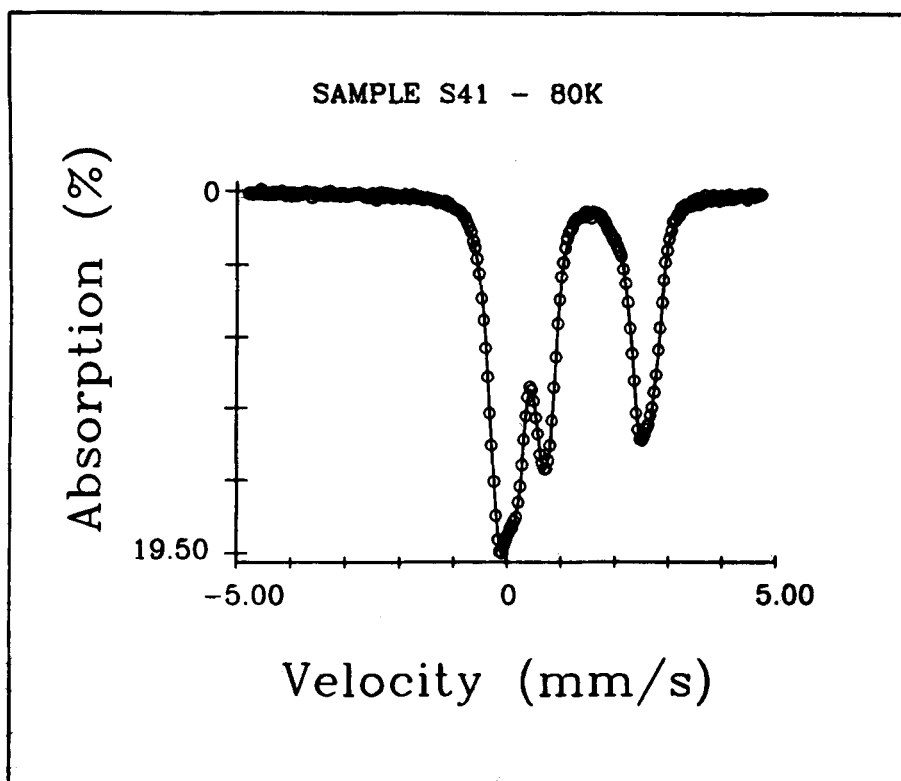


**Figure 3.** Mössbauer spectrum of the S(41) powder sample at 80 K (velocity relative to metallic iron).

**Table 5.** Bond valences for the S(41) iron phosphate (valence units).

	Fe(1)	Fe(2)	Fe(3)	Fe(4)	P(1)	P(2)	P(3)	Sum anion
O(1)	0.26 0.26	0.46			1.20			2.18
O(2)			0.51	0.33	1.20			2.04
O(3)		0.39		0.39	1.22			2.00
O(4)			0.59		1.34			1.93
O(5)		0.43		0.42		1.18		2.03
O(6)			0.46 0.31			1.19		1.96
O(7)		0.40 0.43				1.18		2.01
O(8)	0.44 0.44					1.37		2.25
O(9)	0.23 0.23			0.50			1.24	2.20
O(10)			0.60				1.27	1.87
O(11)			0.40	0.35			1.20	1.95
O(12)		0.59					1.29	1.88
Sum cation	1.86	2.70	2.87	1.99	4.96	4.92	5.00	24.30

The Mössbauer spectrum taken at 80 K (Fig. 3) shows that both ion valences  $\text{Fe}^{2+}$  and  $\text{Fe}^{3+}$  are present. A relative site population of 1.12:2.09:2.30:1.5 was obtained with the fitted spectrum given in Table 4 for iron sites. Mössbauer fitting also showed that for the S(41) sample the relative population of  $\text{Fe}^{3+}$  to the total number of Fe ions is 42.4% ( $x = 2.97$ ), corresponding to the sum of the trivalent site population. The smallest isomer shift (I. S.) value assigned to Fe(4) in Table 4, is consistent with the pentacoordinated Fe(4) site<sup>9</sup>.

The results of the electrostatic balance of cations relative to anions calculated, according to the Brown and Shannon<sup>10</sup> universal curve and Brown and Altermatt<sup>11</sup>, are shown in Table 5. The bond valence ( $s$ ) is calculated from the bond length ( $r$ ) using the equation  $s = \exp [(r_0 - r)/B]$ ,

where  $r_0$  and  $B (= 0.37)$  are empirically determined parameters, many of which have been tabulated. In Table 5, where the Fe(1) and Fe(4) atoms are treated as  $\text{Fe}^{2+}$  ions, we used  $r_0 = 1.734$ . But for the Fe(2) and Fe(3) atoms with mixed valences, we calculated  $s$  using both values for  $r_0$  (1.734 and 1.759). The average value of  $s$  is tabulated in Table 5. In this way, we can attribute different values of  $s$  to the different proportions of  $\text{Fe}^{2+}$  and  $\text{Fe}^{3+}$  ions present in the Fe(2) and Fe(3) sites because their bond lengths  $r$  are between the expected  $\text{Fe}^{2+} - \text{O}$  and  $\text{Fe}^{3+} - \text{O}$  tabulated values.

We would like to propose a way to approximate the proportion of  $\text{Fe}^{3+}$  in the Fe(2) and Fe(3) sites. Let us make  $u$  and  $v$  the proportions of  $\text{Fe}^{3+}$  and  $\text{Fe}^{2+}$ . Thus,  $3u + 2v = (2.70 + 2.87)/2$  from Table 4, and setting  $u + v = 1$  (100%). We find  $u = 0.785$ , that is 78.5% of the four sites of Fe(2)

**Table 6.** Selected parameters of the isostructural series  $\text{Fe}_{7-x}^{2+}\text{Fe}_x^{3+}(\text{PO}_3\text{OH})_{4-x}(\text{PO}_4)_{2+x}$

		S(27)	S(19)	S(41)	S(38)
cell parameters					
a (Å)		7.961	7.977	7.971	7.965
b (Å)		9.611	9.562	9.531	9.516
c (Å)		6.561	6.408	6.389	6.382
alfa (°)		69.19	68.85	68.84	68.73
beta (°)		78.41	78.35	78.40	78.57
gamma (°)		68.01	66.95	66.93	67.00
V(Å <sup>3</sup> )		433.8	418.4	415.4	414.0
$\mu$ (cm <sup>-1</sup> )		61.13	63.38	63.38	64.05
No. of obs. refl.		1030	1112	1299	950
R. index		0.102	0.054	0.050	0.122
Fe(1) = Fe2+	Fe - O av.	2.19	2.18	2.18	2.19
	O - O'av.	3.08	3.08	3.09	3.10
	s Sum	1.79	1.86	1.86	1.83
Fe(2) = mixed	Fe - O av	2.13	2.06	2.04	2.04
	O - O'av.	3.00	2.91	2.88	2.86
	s Sum	2.14	2.57	2.70	2.74
Fe(3) = mixed	Fe - O av	2.12	2.04	2.03	2.02
	O - O'av.	3.00	2.88	2.87	2.86
	s Sum	2.21	2.78	2.87	2.93
Fe(4) = Fe2+	Fe - O av	2.10	2.08	2.08	2.08
	O - O'av.	3.26	3.11	2.85	2.86
	s Sum	1.87	1.96	2.00	1.97
composition	x	0.68	2.7	3.1	3.3
Mössbauer	x	0.46*	2.7	3.0	-
H bond	O(10)...O(12) <sup>G</sup>	2.692	2.764	2.822	2.840

\* S(33) sample.



and Fe(3) of the unit cell are on average occupied by the  $\text{Fe}^{3+}$  ions, i. e.,  $x = 3.1$ , which is in good agreement with Mössbauer spectroscopy ( $x = 2.99$ ).

The anions O(10) and O(12) are electrostatically undersaturated suggesting that they are involved in a possible hydrogen bond. This is corroborated by the distance  $\text{O}(10)\dots\text{O}(12)^{\text{G}} = 2.822 \text{ \AA}$ , and compatible geometry given by the angles  $\text{Fe}(3)^{\text{H}} - \text{O}(10) - \text{O}(12)^{\text{G}} = 103.1^\circ$ ,  $\text{P}(3) - \text{O}(10) - \text{O}(12)^{\text{G}} = 104.6^\circ$ ,  $\text{Fe}(2)^{\text{I}} - \text{O}(12)^{\text{G}} - \text{O}(10) = 97.5^\circ$ ,  $\text{P}(3)^{\text{G}} - \text{O}(12)^{\text{G}} - \text{O}(10) = 109.0^\circ$  that follow from the symmetry operations shown in Table 2.

In Table 6 we show some crystallographic parameters of the four iron phosphate samples, designated as S(27), S(19), S(41) and S(38), and it is possible to see the continuous variation of the parameters with the sample oxidation. The values of  $x$  are linearly correlated to  $1/V$  and in satisfactory agreement with Mössbauer spectroscopy. We think this approximate way of calculating  $x$  can be used even when Mössbauer spectra cannot be obtained.

### Supplementary Material

The list of the observed and calculated structure factors and a stereoscopic view of Fig. 1 is available from the authors (I. Vencato) upon request.

### Acknowledgments

Financial support was received from FUNCITEC, FAPESP and CNPq.

### References

1. E. Mattievich and J. Danon. *J. Inorg. Nuc. Chem.* **39**, 569-580 (1970).
2. G. M. Sheldrick, SHELX76. Program for Crystal Structure Determination. Univ. of Cambridge, England (1976).
3. International Tables for X-ray Crystallography. Vol. IV. Birmingham: Kynoch Press (1974). Present Distributor Kluwer Academic Publishers, Dordrecht.
4. P. Main, S.J. Fiske, S. E. Hull, L. Lessinger, G. Germain, J. P. Declercq, M. M. Woolfson, MULTAN80. A System of Computer Programs for the Automatic Solution of Crystal Structures from X-ray Diffraction Data. Universitys of York, England, and Louvain-le-Neuve, Belgium (1980).
5. C. K. Johnson, ORTEP. Report ORNL-3794. Oak Ridge National Laboratory, Tennessee, USA (1965).
6. P. B. Moore and T. Araki, *Am. Mineral.* **60**, 454-459 (1975).
7. C. Calvo, *Am. Mineral.* **53**, 742-750 (1968).
8. I. Vencato, E. Mattievich and Y. P. Mascarenhas, *Am. Mineral.* **74**, 456-460 (1989).
9. M. G. Clark, G. M. Bancroft and A. G. Stone, *J. Chem. Phys.* **47**, (10), 4250-4261 (1967).
10. I. D. Brown and R. D. Shannon, *Acta Cryst.* **A29**, 266-282 (1973).
11. I. D. Brown and D. Altermatt, *Acta Cryst.* **B41**, 244-247 (1985).
12. I. D. Brown and K. K. Wu, *Acta Cryst.* **B32**, 1957-1959 (1976).